AIChE WILEY InterScience DISCOVER SOMETHING GREAT

Explaining the Enhanced Performance of Pulsed Bioreactors by Mechanistic Modeling

Amaya Franco, Carlos García, Eugenio F. Carrasco, and Enrique Roca
Dept. of Chemical Engineering, School of Engineering, University of Santiago de Compostela, 15782 Santiago de Compostela, Spain

DOI 10.1002/aic.11451
Published online February 29, 2008 in Wiley InterScience (www.interscience.wiley.com).

In this work, steady-state mass balance based models were applied to two UASB reactors and three UAF for a better understanding of the role of pulsation on the efficacy improvement. Models were defined taking into account the hydraulic behavior of each digester and the limiting mechanism of the overall process kinetics (mass transfer or biochemical reaction rate). The application of the model allows to identify that mass transfer was the controlling step in all the reactors, except for the nonpulsed UASB, where methanogenic activity controlled the reactor performance in the last operation steady states. Mass transfer coefficients were higher for pulsed reactors and, in general, a good agreement between those estimated by an empirical correlation and from the model was obtained. Damköhler number values supported that the external mass transfer resistance was not negligible with respect to the process kinetic and in addition, in most cases, it controls the overall process in the reactors. The relative importance of external and internal mass transfer rate was calculated through the Biot number. The values of this dimensionless module indicated that external transport was the main contributor to overall mass transfer resistance. © 2008 American Institute of Chemical Engineers *AIChE J*, 54: 1377–1387, 2008

Keywords: mechanistic model, pulsed flow, anaerobic reactors, mass transfer, hydraulics

Introduction

High-load anaerobic reactors are a wide extended technology for wastewater treatment,[1] since they allowed to obtain high organic loading rates (OLR) and to retain high biomass quantities.[2,3] The high biomass concentrations retained in an anaerobic reactor may be due to bacterial growth on an inert support (fixed and fluidized bed reactors) or by self-immobilization in aggregates or granules (upflow anaerobic sludge blanket, UASB; expanded granular sludge blanket, EGSB; and sequential batch reactor, SBR). However, the development of biofilms with high thickness may increase mass transfer resistance. Therefore, the substrate and the product fluxes within and out of the biomass may become the limiting step, causing important limitations on the overall anaerobic process rate. In fact, for optimizing the organic load, it is necessary to find the equilibrium between high biomass concentrations, granule/particle size, and the mass transport limitations that may be produced in the sludge bed.[4]

In other work,[5] it was found that the only parameter which affects the COD removal in UASB reactors would be the nutrients mass transfer when the influent concentration was high. These authors observed that the substrate flux through a biofilm or granule is proportional to the concentration gradient between the surface and the inner layer. Based on this, bacteria within the granule will have a minor activity, as they are exposed to a lower substrate concentration. Relative importance of mass transfer depends on specific activity, K_m value, bulk substrate concentration and biofilm thickness (or granule diameter).

Correspondence concerning this article should be addressed to E. Roca at eqeroca@lugo.usc.es.

Dolfing (1985)[6] investigated the influence of mass transfer limitations with low substrate concentrations by determining the apparent K_m values. The effect of mass transfer resistance was only important when working with low substrate concentrations and with biofilms of high methanogenic activity, conditions that can be found in high-load anaerobic reactors. The results obtained in several research works about this effect on anaerobic biomass are contradictory. Some authors affirm that external and internal mass transfer resistance influences the substrate consumption rate,[6–10] while others did not observe mass transport limitations in this type of biomass.[11,12] In fact, pH gradient within the granule would have more influence on the conversion rate than mass transfer resistance.[12]

It has been found that external mass transport resistance (liquid–solid) was negligible in denitrifying filters[13] and, in theory, in methanogenic biofilms with a thickness lower than 1 mm[14] and in fixed bed bioreactors with aggregates higher than 2 mm.[15] In another work,[10] external mass transfer was practically null operating at upflow velocities higher than 1 m/h. However, limitation on external mass transfer in UASB reactors was found, although it was negligible in EGSB reactors.[9] Wu et al. (1995)[8] studied the influence of mass transfer between the bulk liquid and the granule wall at different agitation rates, finding a high resistance to mass transport operating at low velocities (200–400 rpm). Similar results were obtained in an EGSB, where a better operation was produced when the upflow velocity was increased to 14 m/h.[16] Furthermore, it is important to distinguish whether the percentages of COD removal increased due to a decrease of mass transfer resistance or due to the elimination of shortcuts in the sludge bed (avoiding non ideal flow behavior), since gas production is the main factor enhancing mixing in anaerobic reactors. Mass transfer resistance was studied by determining the values of the transfer coefficient at several upflow velocities.[17] It was observed that transport resistance between phases decreased exponentially as the upflow velocity increased.

On the other hand, mass transfer rate in a granule should be related with both porosity and size distribution of pores within the granule.[18] Another important factor that might influence internal mass transfer is the granule diameter. In fact, granule size has a greater influence on the apparent affinity constant, which increases with the particle diameter.[10] These results indicate the existence of mass transfer limitations in anaerobic granules. Nevertheless, other studies have leaded to opposite results. No relation was found between the affinity constant and the granule diameter, something expected if it is taken into account that only the outer layer of the granule was active.[19] In another study,[11] the same acetoclastic methanogenic activity in both intact and disintegrated granules was observed, although very small granules (0.44 mm) were employed.

It was observed that specific granule configurations might have a positive influence in the substrate conversion rate. For example, a cluster disposition of the different trophic groups may offer a lower limitation to mass transport[20] than a layered structure.[21] A sludge bed constituted by small size particles presents a high biological active surface, from the point of view of substrate penetration and transformation. Therefore, the apparent reaction rate in a bioreactor may be limited by both the biological activity of the biomass and by the mass transfer resistance between phases.

The above-mentioned studies confirm that mass transfer limitations may exist in anaerobic biofilms. However, this process will only be the limiting step when: (a) substrate concentration in the reactor is low, (b) the percentage of granules with an average diameter greater than 1 mm is high, and (c) methanogenic activity of biomass is high, since the normal value varies between 0.4 and 0.6 kg COD/kg VSS·d.[22]

Pulsing flow has been applied to a great number of chemical[23–25] and biochemical processes[26–28] for improving mass transfer, performance, and efficiency of the equipment employed. Pulsing flow allows removal efficiency and stability to be improved in upflow anaerobic filter (UAF) and UASB reactor, as it favors degasification and decreases the formation of preferential pathways.[29–31] Besides, it also favors biomass aggregation and granule development in UASB reactors.[29,30]

In this work, the key mechanisms and parameters involved in the enhancement of the performance of pulsed anaerobic reactors are investigated. Steady-state mass balance based models were applied to better understand the role of pulsation on the efficacy improvement of UASB reactors and UAF. The identification of the model parameters for fitting the experimental data obtained with pulsed and nonpulsed systems could support the phenomenological behavior observed and the advantages that pulsation introduces in the operation of anaerobic reactors.

Materials and Methods

Bioreactors

Experimental data of the operation, hydraulic behavior and biomass characteristics of UASB reactors,[30] and UAF[31] were employed for the development and validation of mechanistic models, and for the calculation of dimensionless numbers. The models were applied to three UASB reactors and two UAF. Two of the UASB reactors (P1 and P2) and one of the UAF (P2) were operated with pulsing flow (this notation is the same used in the referenced papers), while in both cases, one of the reactors was operated without pulsation (NP) for comparison. Pulsing flow was produced by an elastic membrane pulsator (EMP),[32] placed in the bottom part of reactors P1 and P2s. The EMP consists of a system formed with one or more elastic tubes coupled to an electrovalve, being its aperture controlled by a timer. Pulsation within the column of the reactor is provoked by the liquid retained inside the elastic tube/s when the valve is closed, which is propelled within the reactor when the valve is opened. Pulsation in reactor P1 was generated by pulsing simultaneously the feeding and the recycling flow, while in reactors P2 (UASB and UAF), only the feeding flow was pulsed, since they were operated without recycling. This difference conditioned not only the frequency and the amplitude of pulsation, but also the upflow velocity of each reactor.[30]

In Table 1, the closing time of the electrovalve (t_s), the frequency of pulsation (f_p), the pulsed volume/reactor volume ratio (V_p/V_r) (which is responsible for the mechanical effect

Table 1. Closing Times (t_s), Pulsation Frequencies (f_p), Pulsed Volume/Reactor Volume Ratio (V_p/V_r) and Upflow Velocity (v) of UASB Pulsed Reactors (P1 and P2) and UAF P2

Reactor	t_s (s)	f_p (s^{-1})	V_p/V_r	v (m/s)
UASB P1	200	4.9 E −03	1/27.5	3.07 E −05
UASB P2	1,800–900	(1.4–11.0) E −04	1/230–1/60	7.1 E −07 to 1.4 E −06
UAF P2	1,800–900	(1.4–7.0) E −04	1/230–1/60	(1.48–7.62) E −06

of pulsation), and the upflow velocity achieved in each case are shown. In reactor P1, these three parameters were kept constant by regulating the recycling flow as the feeding flow increased, while in the two reactors P2, the V_p/V_r ratio and thus, the pulsation amplitude and the upflow velocity, changed depending on the loading rate. UASB reactors and UAF volume was the same (0.8 L). UAFs were filled with 120 corrugated PVC Raschig rings of 12 mm in size, decreasing their overall volume from 0.80 to 0.76 L.

Inoculum

The inoculum of both UASB reactors and UAF came from a hybrid UASB-UAF reactor treating dextrose, although it was collected at different times. In case of the UASB reactors, the inoculated biomass was in granular form and with a specific methanogenic activity (SMA) of 0.27 kg COD-CH_4/kg VSS·d, whereas for UAF the sludge was flocculent, with a SMA of 0.2 kg COD-CH_4/kg VSS·d. The final volatile suspended solids (VSS) concentration in each reactor was in a range of 14–15 g/L.[30,31]

Hydrodynamic behavior

The hydrodynamic behavior of UASB reactors and UAF was considered according to a characterization carried out previously.[30,31] In those works, a stimulus-response technique was used to determine residence time distributions (RTD) and, from this, the hydrodynamic behavior of the system. Dextran blue and LiCl were simultaneously employed as tracers, to obtain the useful working volume, the volume occupied by biomass, and the void volume of the sludge bed in the reactors. The first tracer is more adequate for determining the useful liquid volume of the reactors and the biomass volume, and the latter is obtained by the difference between theoretical hydraulic residence time (HRT) and dextran blue HRT, because its high molecular size impedes its penetration inside microporous structure. However, LiCl enters through very small cavities, thus allowing the determination of the void volume fraction of biomass (as the difference between HRTs obtained with dextran blue and LiCl).[30]

Description of the model

Model Simplifications and Approaches. Modeling of the reactors was established considering the following theoretical approaches and simplifications: (1) The limiting phase of anaerobic degradation is always methanogenesis; (2) Particles or granules which constitute the sludge bed have spherical geometry; (3) The liquid–solid interphase thickness is very small and not much variable despite changes in the upflow velocity; (4) Growing of biomass within the reactor is exponential, assuming unlimited substrate availability; (5) The substrate concentration within the particles/granules is negligible with respect to the concentration in the outer layer; (6) The sludge bed keeps constant its geometry during the whole nonpulsed operation.

The developed models are based on mass balances. For establishing these balances, the hydraulic behavior and the limiting mechanism of the apparent reaction rate were considered. The latter may be due to mass transfer between phases or to the biological reaction rate.

Statement number 5 was assumed taking into consideration that these bioreactors are in general well agitated systems, especially at moderate-high loads, like those applied in this work. Therefore, it can be reasonably assumed that concentration in the bulk liquid is almost equal to the concentration in the outer layer of the granule. Consequently, it can be considered that concentration in the inner part is negligible, since there are evidences in literature[19,33] that mentioned an inert zone in the core of the granules. This is caused because substrate does not reach deep layers, causing bacterial death by starvation.

Modeling of UASB and UAF Bioreactors. The generic mass balance applied to UASB reactors and UAF is described by Eq. 1:

$$r_a = Q_0 S_0 + Q_r S_f - (Q_0 + Q_r) S_f \tag{1}$$

where S_0 is the initial substrate concentration (kg COD/m^3), Q_0 is the feeding flowrate (m^3/d), Q_r is the recycling flowrate (m^3/d), S_f is the final substrate concentration (kg COD/m^3), and r_a is the apparent substrate consumption rate (kg COD/d).

To better understand the different observed behavior of all reactors, a mathematical model taking into account the different aspects (kinetics, external mass transfer, and hydraulics) was developed.

Apparent kinetics: The apparent substrate consumption rate (r_a) may be due to two different mechanisms. One of them would be the biological reaction rate of methanogenic bacteria (the slowest phase of the whole anaerobic degradation process and therefore the one conditioning the overall rate), because the substrate employed (dextrose) for feeding the reactors was not complex and only acidogenesis and methanogenesis were involved in its degradation. The biological reaction rate (r_a) can be calculated from SMA measures and from the kinetics of bacterial growth. Once r_a is known, the final substrate concentration is calculated from Eq. 2:

$$S_f = \frac{Q_0 S_0 - r_a}{Q_0} \tag{2}$$

External mass transfer: Another limiting step may be the mass transfer from the liquid to the particles/granules, where the substrate transformation into CH_4, CO_2, and H_2 is mainly done. In this case, the apparent reaction rate is calculated by the expression described by Eq. 3:

Table 2. Model Parameters in UASB Reactors (NP, P1, and P2) and UAF (NP and P2)

Reactor	V (L)	ε (−)	Weighted Particle Diameter d_p (mm)		Total Number of Particles		Overall Surface of Particles (m^2)	
UASB								
NP	0.53	0.415	1.173		3.19×10^5		1.362	
P1	0.59	0.424	1.153		2.62×10^5		1.131	
P2	0.64	0.469	1.010		2.97×10^5		0.925	
UAF			Granular	Flocculent	Granular	Flocculent	Granular	Flocculent
NP	0.54	0.431	1.173	0.12	6.45×10^4	5.98×10^7	0.278	2.706
P2	0.68	0.141	1.010	0.12	9.44×10^4	5.50×10^7	0.298	2.489

$$r_a = k_L A S_f \tag{3}$$

where k_L is the mass transfer coefficient referred to the outer granule surface (m/d) and A is the liquid/granule area of mass exchange (m^2).

Then, the final substrate concentration S_f in the reactors is calculated by the equation:

$$S_f = \frac{Q_0 S_0}{Q_0 + k_L A} \tag{4}$$

Hydraulics: Data obtained from RTD curves have indicated that the UASB NP reactor presented a hydraulic behavior very close to a CSTR (Continuous Stirred Tank Reactor), while UASB P1 and UASB P2 pulsed reactors behaved like 1.26 and 1.9 CSTR coupled in series, respectively.[30] Using the same stimulus-response technique described earlier, data obtained from RTD curves show that the UAF NP and UAF P2 reactors behaved like 1.7 and 2.21 CSTR coupled in series, respectively.[31] Thus, according to their hydraulic behavior, UASB reactors and UAF were divided into two compartments (zones 1 and 2), except reactor UASB NP, which was not divided, and UAF P2, which was divided into three compartments. Therefore, the volume is divided so that zone 2 represents the $N-1$ volume of the zone 1 volume, N being the number of ideal CSTR obtained from RTD curves. If the limiting mechanism in the reactors is biological reaction then the mass balance would be the one described by Eq. 2, applied to each zone. However, if mass transfer rules the apparent substrate consumption rate then the mass balance in the zone 1 of reactors with recycling flow (UASB P1 and UAF NP) is described by the following expression:

$$S_a = \frac{Q_0 S_0 + Q_r S_f}{Q_0 + Q_r + \frac{k_L A}{N}} \tag{5}$$

where S_a is the substrate concentration at the outlet of zone 1 (kg COD/m^3). In this case, the exchange area of zone 1 must be the total exchange area divided by N, since a uniform particle distribution size in the whole reactor is assumed. In the zone 2, the balance takes the form:

$$S_f = \frac{S_a (Q_0 + Q_r)}{Q_0 + Q_r + \frac{k_L A}{N}(N-1)} \tag{6}$$

The global mass balance in these reactors is obtained by replacing the S_a value in the Eq. 6:

$$S_f = \frac{(Q_0 + Q_r)(Q_0 S_0 + Q_r S_f)}{\left(Q_0 + Q_r + \frac{k_L A}{N}\right)\left(Q_0 + Q_r + \frac{k_L A}{N}(N-1)\right)} \tag{7}$$

However, reactors UASB P2 and UAF P2 have no recycling flow, and therefore, only the feeding flow is pulsed. If the controlling mechanism is mass transfer, and following the same procedure above-mentioned, then the global mass balances in reactors UASB P2 and UAF P2 are described by Eqs. 8 and 9, respectively:

$$S_f = \frac{Q_0^2 S_0}{\left(Q_0 + \frac{k_L A}{N}\right)\left(Q_0 + \frac{k_L A}{N}(N-1)\right)} \tag{8}$$

$$S_f = \frac{Q_0^3 S_0}{\left(Q_0 + \frac{k_L A}{N}\right)^2\left(Q_0 + \frac{k_L A}{N}(N-1)\right)} \tag{9}$$

Model Parameters. Implicit parameters involved in the mass balance were calculated from experimental data of each reactor.[30,31] The useful volume (V) and the porosity (ε) of the sludge bed were determined from RTD assays employing dextran Blue and LiCl as tracers, as mentioned in Materials and Methods section. The average diameter of granules d_p was determined by doing a weighted mean of particle size distribution data. For determining the size distribution of biomass, a similar method to that described in Jeison and Chamy (1998)[34] was employed. The granule samples were fixed in agar solution (5 g/L) on a Petri dish, and once immobilized, an 8-bit gray scale image was obtained by scanning the sample. This image was analyzed by the software UTHSCSA Image Tool, which was developed by Texas University (Health and Science Center).

In UAF, a mixture of granular and flocculent sludge was developed. Thus, the average particle diameter has not been determined experimentally due to the difficulty of measuring the diameter of flocculent particles. Average diameter of this kind of particles was supposed to be uniform and equal to 0.12 mm.[35] On the other hand, the average diameter of granular particles d_p can be considered similar to that obtained for UASB reactors. The number and the total external area of particles (granules) in both UASB reactors and UAF are calculated assuming a spherical geometry. The values of the calculated parameters in each reactor are shown in Table 2.

SMA values of the biomass were needed for model and dimensionless numbers calculations. Thus, values of the SMA employed for UASB reactors were in accordance with those presented in the experimental data[30]. However, for UAF, the SMA of the biomass was calculated as an average of the initial and final values, since it was only measured at the beginning and at the end of the operation.

Calculation Procedure of the Model. The mathematical models which described the performance and behavior of the UASB reactors and UAF were implemented in Matlab® and

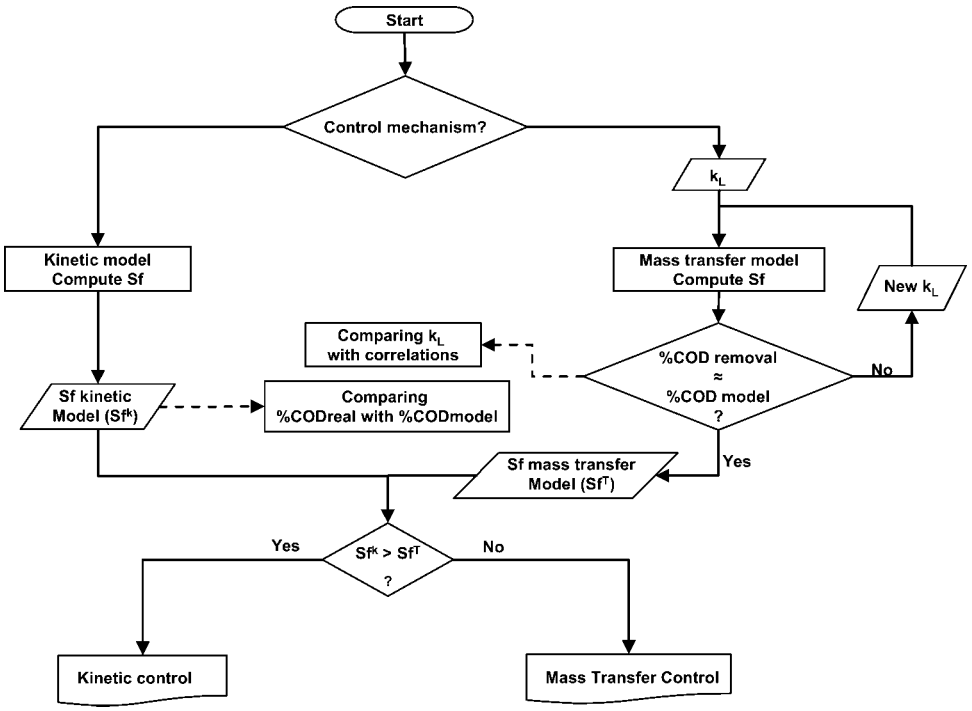

Figure 1. Flow sheet of the simulation procedure.

run iteratively. The model simulation procedure is shown in Figure 1. The aim of the first model simulation was to find out the mechanism that was driving the overall process rate in each reactor for the different quasi-steady state periods considered. With that aim, the final concentrations obtained by the two mechanisms were compared and the mechanism which estimates the highest final concentration was chosen.

Subsequently, the model was adjusted for the calculation of the mass transfer coefficient (k_L) or the biological reaction rate, depending on the mechanism controlling the overall process rate. Once these parameters were calculated, a subsequent simulation was performed to check the correct adjustment of the previous simulation, and to obtain the definitive results.

Data for five quasi-steady state periods in UASB reactors and UAFs were employed as input to the model. Standard deviation lower than 2 for the OLR (kg COD/m^3 d) and than 4 for the percentage of COD removal was considered as criteria for selecting the quasi-steady states periods. OLR applied and their standard deviations for UASB reactors and UAF, respectively, are shown in Tables 3 and 4.

Results and Discussion

Model application

The proposed model was applied for fitting the experimental data of the different reactors to better understand their performance with or without pulsing flow.

UASB Reactors. The results obtained by running the model for the nonpulsed UASB reactor show that the controlling mechanism in the first two periods was mass transfer, whereas the biological reaction rate ruled in the remaining ones. Thus, the value of the k_L was calculated with Eq. 4 and using experimental data of COD removal.

The limiting mechanism in the pulsed reactors (P1 and P2) for all the steady states was mass transfer. The values of the mass transfer coefficient (k_L) for each reactor were calculated employing Eqs. 7 and 8, in a similar way as for NP reactor.

Once the mass transfer coefficients or the reaction rate (depending on the limiting mechanism) were calculated in each reactor, the goodness of the model for fitting the experimental data was evaluated. Figure 2 shows the experimental percentage of COD removal (plus standard deviation) and the percentage estimated by the model for each reactor. As it

Table 3. Quasi-Steady State OLRs Values Employed for the Model Fitting in UASB Reactors

Period (d)	NP (kg COD/m^3 d)	P1 (kg COD/m^3 d)	P2 (kg COD/m^3 d)
10–20	2.86 ± 0.08	2.84 ± 0.19	2.41 ± 0.24
42–46	1.77 ± 0.035	3.91 ± 0.42	4.73 ± 0.04
56–65	3.89 ± 0.24	7.16 ± 0.26	7.16 ± 0.46
81–94	4.44 ± 0.29	7.70 ± 0.44	8.25 ± 0.16
109–123	6.12 ± 0.20	11.86 ± 0.51	12.03 ± 0.85

Table 4. Quasi-Steady State OLRs Values Used for Model Fitting in UAFs

Period (d)	NP (kg COD/m^3 d)	P2 (kg COD/m^3 d)
9–15	2.53 ± 0.26	2.78 ± 0.22
30–45	4.07 ± 0.37	4.34 ± 0.26
50–70	5.86 ± 0.38	6.86 ± 0.39
70–90	7.28 ± 0.62	9.09 ± 0.86
104–118	10.88 ± 0.80	14.28 ± 0.28

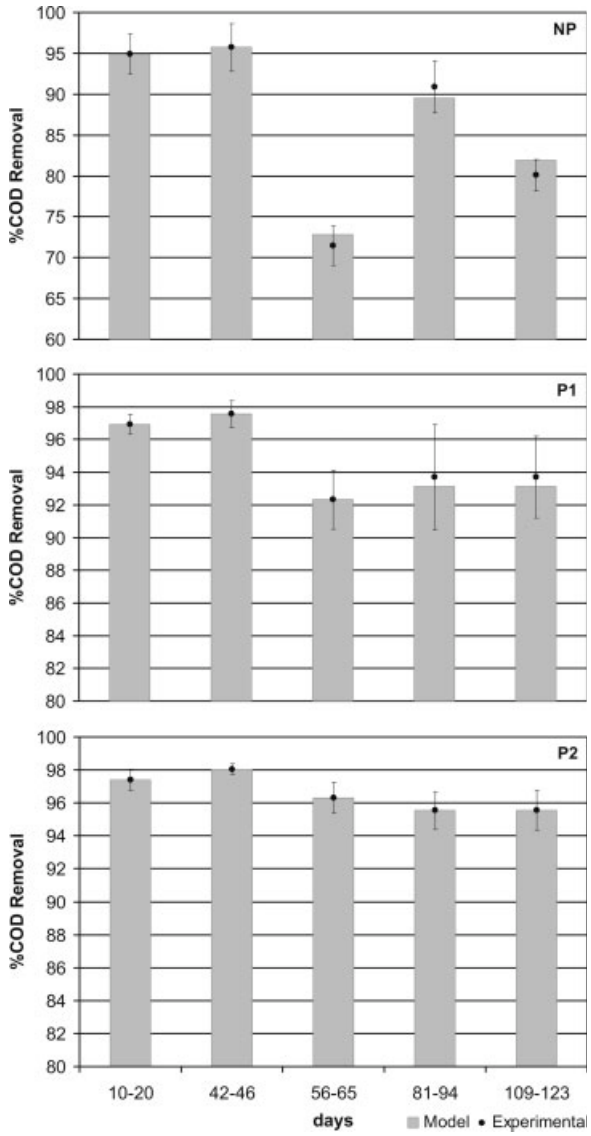

Figure 2. Experimental data of NP, P1, and P2 UASB reactors fitted by the model.

can be seen in the graphs, the model reproduces quite well the behavior of the three UASB reactors, this indicating that the selection of limiting mechanisms by the model was adequate in each steady state. Thus, in reactor NP, mass transfer was the limiting mechanism in the first 46 days of operation. This behavior is in accordance with experimental data, since the elimination efficiency in this period was high and the reactor did not show any limitations in the biological reaction rate. However, from that moment, the reactor performance was not good, achieving poor removal efficiencies, although the applied load was not very high in the last three steady states. SMA was decreasing progressively until the end of the operation, as it is also explained by the model, which indicated the biological reaction rate as the limiting mechanism during these periods. In pulsed reactors, the limiting mechanism indicated by the model was mass transfer rate. In these reactors, the operation was stable most of the time, presenting both good removal efficiency and a high methanogenic activity, in agreement with model results.

UAF. In this case, the limiting mechanism in all the steady state periods for both NP and P2 reactors was mass transfer. Model results agree quite well with the operation data. The operation efficacy of these reactors was good during the whole experimentation, especially for reactor P2, which achieved higher removal efficiencies at higher loads than those used in reactor NP. The k_L coefficients were estimated using Eqs. 8 and 9 (with and without recycling), and then, the experimental data was fitted by the model. Once again, and as it can be seen in Figure 3, the fit goodness is very high for the two reactors in all the steady state periods. The model explains good enough the reactor performance, thus, the mechanistic approach is adequate.

Comparison between model-estimated and correlation-estimated mass transfer coefficients

With the aim of supporting the results obtained from the model, external mass transfer coefficients determined by the model were compared with those estimated using correlations available in the literature. The value of the external mass transfer coefficient depends on the physical properties of the liquid, the diameter of the particle, and the hydrodynamic conditions of the surrounding environment. Several relationships for the estimation of k_L are presented in the literature. In most of them, the mass transfer coefficient is determined by the Sherwood number (*Sh*), as a function of the Reynolds number (*Re*), and the Schmidt number (*Sc*). In this case, the selected relationship employed for the estimation of k_L was the one presented by Eq. 10[36]:

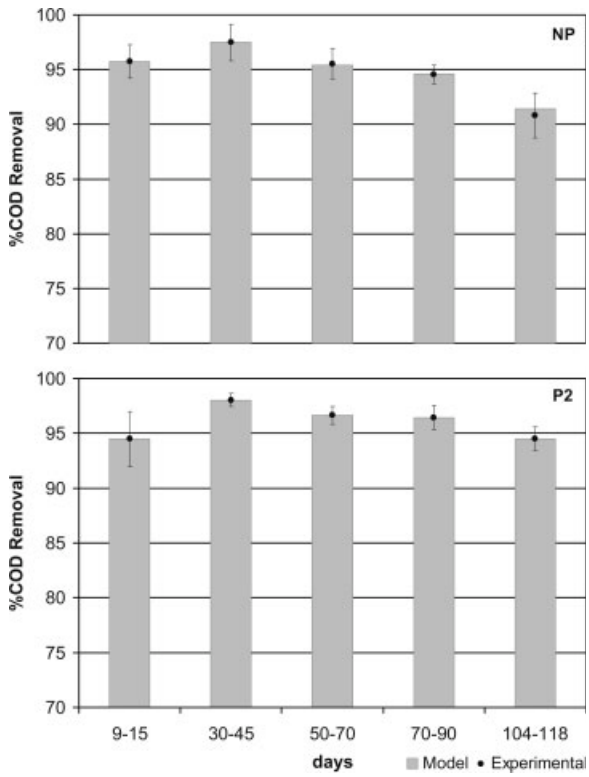

Figure 3. Experimental data of NP and P2 UAF fitted by the model.

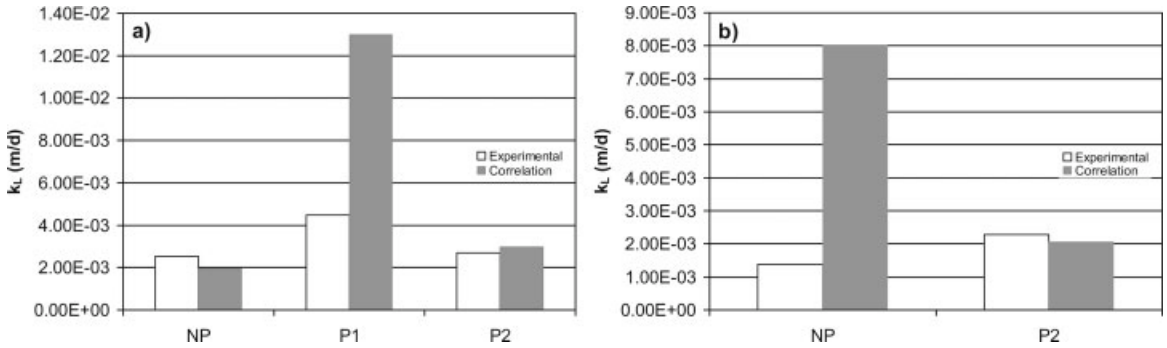

Figure 4. Average external mass transfer coefficient for (a) UASB and (b) UAF.

$$Sh = \frac{k_L \cdot d_p}{D_e} = 1.90 \cdot Re^{1/2} \cdot Sc^{1/3} \cdot \varepsilon \cdot (1-\varepsilon)^{1/2} \quad (10)$$

$$Sc = \frac{\mu/\rho}{D_e} = \frac{\upsilon}{D_e} \quad (11)$$

$$Re = \frac{v \cdot d_p \cdot \rho}{\mu} = \frac{v \cdot d_p}{\upsilon} \quad (12)$$

where D_e, υ, d_p, v, and ε are the effective diffusivity (m^2/s), the kinematic viscosity (7.24 E −07 m^2/s, water at 35°C[36]), the average diameter of particle (m), the upflow velocity (m/s), and the porosity of the sludge bed, respectively. D_e was assumed as the diffusion coefficient in water (5.79 E −11 m^2/s) since a suitable method for estimating D_e in biological biofilms under these experimental conditions is not available.[37] The values employed for d_p and ε are shown in Table 2, while values of $v(V_a)$ are shown in Table 1 for each reactor.

Although experimental mass transfer coefficients were determined for each steady state in both UASB reactors and UAF, in Figure 4, only the average experimental values of the k_L are shown for comparison purposes with the theoretical k_L for each reactor. In general, a good agreement is obtained between the values estimated from the model and the generalized correlation, except for UAF NP and UASB P1 reactors. In the UAF, the theoretical k_L for NP is four times higher than for P2. This is mainly due to the higher porosity of the sludge bed in the nonpulsed reactor, which may theoretically lead to an improvement in the mass transfer rate. However, the porosity of NP reactor could be overestimated due to the presence of a higher proportion of gas bubbles entrapped in the sludge bed. A lower value of the useful volume (and thus higher biogas accumulation) in the NP reactor was also observed.[31] The effective mass transfer area was significantly decreased by biogas retention and the presence of shortcuts in the sludge bed, as can be observed in Figure 5. This nonideal behavior generates a bad contact between phases and a high decrease in the mass transfer rate. This explains the low experimental value obtained and the difference between the experimental and the theoretical coefficients (8 times). Model and correlation estimated k_L were almost equal in reactor P2, being the experimental value twice higher than in the nonpulsed reactor, this proving the efficiency of pulsing flow for enhancing mass transfer in fixed bed reactors. Regarding UASB reactors, P1 presented the highest value of the experimental k_L (4.49 E −03 m/d), while NP and P2 presented similar values (2.54 E −03 and 2.71 E −03 m/d, respectively).

Much higher values of local mass transfer coefficients were obtained in biofilms (from 0.36 to 0.64 m/d), although upflow velocities as high as 56 m/h were applied.[38] However, it has to be considered that these velocities are difficult to apply during normal operation conditions of bioreactors, including EGSB. In the present case, comparable to these values are the maximum values of the mass transfer coefficient during a pulse in UASB P1, UASB P2, and UAF P2, which were 0.18, 0.12, and 0.074 m/d, respectively. These values give an idea of the high punctual upflow velocity applied and the mixing effect and shear stress provoked in pulsed reactors.

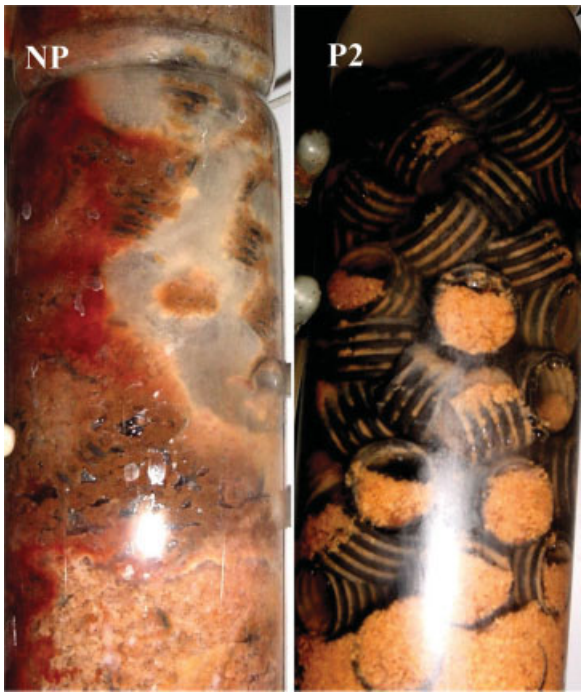

Figure 5. Photographs of the sludge bed of UAF NP and UAF P2.

[Color figure can be viewed in the online issue, which is available at www.interscience.wiley.com.]

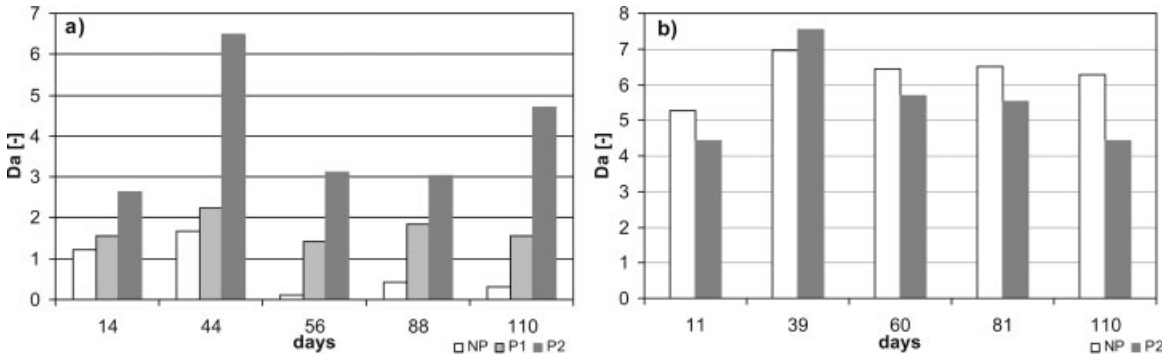

Figure 6. Damköhler number values in each steady state for (a) UASB reactors and (b) UAF.

This higher value of k_L in reactor P1 (especially the estimated by correlation) can be related with the higher upflow velocity. The significant disagreement between the experimental and the theoretical k_L in this reactor can be explained by the high upflow velocity applied. This fact provoked a hydraulic stress and the formation of denser granules with a compact structure, more likely to resist the high shear stress imposed, similarly to what occurs in biofilms.[39] As a consequence, the value of the experimental mass transfer coefficient diminished.

Dimensionless numbers

As it was demonstrated, mass transfer has a key role in the improved performance of UASB reactors and UAF when they are pulsed. To better illustrate the effect of mass transfer on the overall substrate removal rate in UASB reactors and UAF (pulsed or non pulsed), two dimensionless modules have been calculated, the Damköhler number (*Da*) (i.e., the ratio of the maximum kinetic rate to the maximum external mass transfer rate) and the Biot number (*Bi*) (i.e., the ratio of the external mass transfer rate to the internal mass transfer rate).

Kinetic vs. External Mass Transfer Rate. Assuming quasi-steady state conditions, no substrate accumulation is produced on the granule surface, and therefore it is necessary that the substrate transport rate be equal to the substrate consumption rate by biochemical reaction on the biocatalyst surface. Based on a kinetic type of Monod, the Damköhler number is established by Eq. 13.[40]

$$Da = \frac{r_{\mathrm{m}}}{k_L \cdot S_{\mathrm{f}}} = \frac{\text{max. kinetic rate}}{\text{max. external mass transfer rate}} \qquad (13)$$

Damköhler number relates the maximum reaction rate with the maximum external mass transfer rate. Values of *Da* higher than 1 indicate that the studied system is limited by external mass transfer, which will be the slowest process step, while values of *Da* lower than 1 indicate a system controlled by reaction rate. The values of *Da*, estimated from the experimental data (Figure 6), allow concluding that the external mass transfer resistance was not negligible with respect to the process kinetic and in addition, in most cases, it controls the overall process in the reactors. The greater influence of external mass transfer on substrate consumption rate has also been observed in other investigations.[8,9,16,17,41] As it can be seen in Figure 6a, pulsed UASB reactors always presented higher values of the *Da* number, especially P2, which was in general significantly higher than those obtained in the other reactors. In the pulsed reactors the *Da* indicates control of mass transfer, while in the UASB NP reactor the *Da* values lower than 1 in the last three steady states indicate kinetics as the limiting mechanism, being these results in agreement with those obtained by the model. UASB reactors were mainly developed[3] with the aim of solving the problems traditionally associated with anaerobic filters (i.e. mass transfer resistance, formation of preferential pathways...). Thus, the configuration of UASB reactors allows an important decrease in mass transfer resistance with respect to UAF (this can be observed in the higher values of *Da* in Figure 6b). The main problem in UASB reactors is the development of a sludge bed with good characteristics, since depending on the wastewater, granules may present bad properties.[42] Here, the positive effect of pulsing flow was evidenced by the *Da* number values. Pulsing flow promotes the formation of a granular sludge bed with higher porosity and lower d_{p} (especially in P2), which increases the active surface of the biomass and, consequently, increases the SMA.[33] Therefore, the controlling mechanism is always mass transfer, as *Da* values showed that the proportional effect of the biochemical reaction rate is significant. Higher values of the *Da* number in reactor P2 are a consequence of the higher SMA with respect to reactor P1. Besides, k_L values in reactor P1 were higher, this also contributes to the lower values of the *Da*, although it has to be taken into account that this reactor was neither controlled by biological reaction.

As above-mentioned, UAF has higher values of the *Da* number, since this type of reactors usually present mass transfer problems due to the clogging of the sludge bed, caused by an excessive biomass growth on the media support. Therefore, pulsation was mainly applied to UAF to decrease mass transfer resistance and avoid the formation of preferential pathways. In Figure 6b an increase of the values of *Da* in the second steady state, according to the biomass growth and the poor biogas production at this time, can be observed. However, as the OLR was increasing, the *Da* number of UAF P2 was decreasing progressively until the initial value due to an important increase in the k_L (3.64 E −03 m/d), which was 2.6 times higher than that in the UAF NP (1.40 E −03 m/d). The increase in the mass transfer coefficient was obtained by the high upflow velocity applied at high OLR, favoring degasification, promoting a uniform distribution of biomass through the media support and avoiding

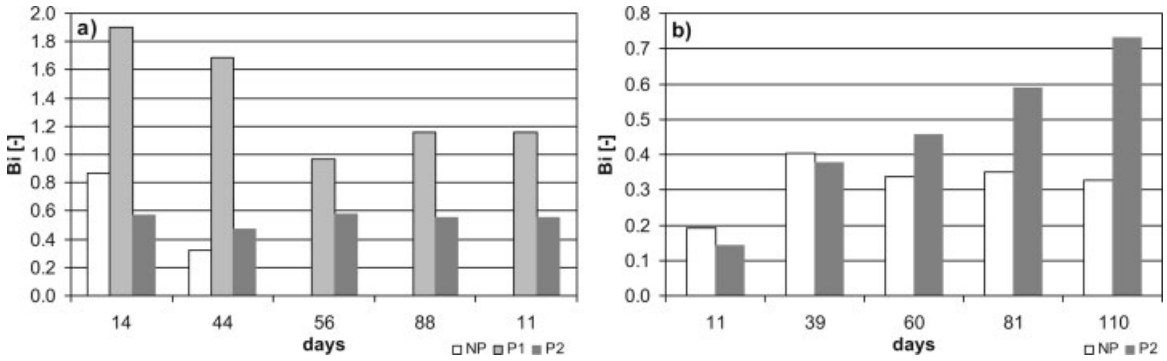

Figure 7. Biot number values in each steady state for (a) UASB reactors and (b) UAF.

the formation of sludge compacting. In the nonpulsed reactor, *Da* value did not almost vary in the last three steady states (around 6.5) due to the continuous presence of gas retention and clogging of the bed (Figure 5).

External vs. Internal Mass Transfer in Granules. Some authors have found limitations to internal mass transfer in biofilms,[6,8–10,43] thus it is interesting to evaluate the relative importance between the effects of internal diffusion and external mass transfer. The Biot (*Bi*) number[44] is used to compare the internal and external mass transfer like the quotient between velocities of both phenomena. Values of the Biot number higher than 100 imply[40] that the external mass transfer is negligible. On the contrary, if *Bi* is low then the internal mass transport resistance is unimportant.

$$Bi = \frac{k_L \cdot d_p}{D_e} = \frac{\text{external mass transfer rate}}{\text{internal mass transfer rate}} \qquad (14)$$

According to Brito and Melo (1999),[45] imposing changes in the hydraulic regimen of a reactor with a well developed biofilm may improve the internal mass transfer coefficient, possibly due to an additional convection effect.[45] In fact, several authors have observed experimental evidence of convective fluxes within biofilms mainly due to pressure gradients.[46–48] In pulsed reactors, internal mass transfer should then be negligible, since the flow regime is suddenly changed when the pulse is produced. As it can be observed in Figure 7, neither UASB reactors nor UAF presented *Bi* number values greater than 100 and therefore the external mass transfer is controlling the process in both UASB reactors and UAF (pulsed or not pulsed). However, the evolution of this dimensionless number through the steady states may indicate differences between the reactors, as in the case of *Da* number (note that Biot number is not calculated for reactor UASB NP in the last three steady states because of reaction rate control).

As it can be observed in Eq. 14, the numerator of the *Bi* number is influenced by the external mass transfer coefficient and the particle diameter. UASB P1 reactor presents the higher values of the *Bi* number. This reactor contains the particles with a high diameter and the higher k_L, due to the upflow velocities applied. Pulsed volume (and mechanical effect) was higher in reactor P1 than in reactor P2, and the biocatalyst presented a higher size and a lower porosity in the first one, this being a response of the biofilm (in this case, granules) to stand the higher hydraulic stress. However, as it was previously shown,[49] pulsation may have an optimum frequency that leads to the best results in the operation of bioreactors and to the formation of biomass aggregates with optimum characteristics. In reactor P2, pulsation was generated each 900–1800 s, allowing the production of biogas between pulsations and its sudden release when the pulsation was produced, this provoking an important stress caused mainly by biogas, which favors the formation of small-size granules,[50] very active.[33] Therefore, *Bi* numbers are lower in this reactor. This difference in the *Bi* number between P1 and P2 reactors agrees in a certain manner with the work of Beyenal and Lewandowski (2002).[44] These authors stated that aerobic biofilms grown at low flow velocities exhibit low density and high effective diffusivity but cannot resist higher shear stress, whereas biofilms grown at higher flow velocities are denser and can resist higher shear stress but have a lower effective diffusivity. However, in this case, reactor P2 presented small granules with high specific density, strength, and porosity, which were formed due to the particular effect (liquid + biogas shear stress) of low frequency pulsation. In UAF, *Bi* number is higher in P2 than in NP, this being in accordance with the results obtained with the *Da*.

Conclusions

A mechanistic model was proposed to better explain and elucidate the controlling mechanisms in two types of anaerobic reactors (UASB and UAF), operated under different hydraulic conditions (pulsed and nonpulsed flow). Model results indicated that mass transfer controlled in most occasions the performance of the five studied reactors, this being supported by the values obtained of *Da* number. However, the reason why mass transport is always the limiting mechanism is different and it depended on the type of biomass, reactor configuration, and hydraulic regimen. Therefore, *Da* numbers calculated in UAF were higher than in UASB reactors, this indicating the significant magnitude of mass transfer resistance traditionally associated with fixed bed systems. Thus, the k_L value on the pulsed UAF was more than twice higher than in the NP, this proving the efficiency of pulsations for decreasing mass transfer problems in this type of reactors. On the other hand, *Da* values for the pulsed UASB reactors were higher than the nonpulsed one. This was mainly supported not on a significant difference in the k_L coefficients but in the properties of granules, which were of lower size and

more active. Thus, mass transfer resistance became the limiting mechanism not because of its high magnitude but because of the high activity of the sludge bed in pulsed reactors, especially in reactor P2. Finally, external mass transport (between the bulk liquid and the granule surface) was identified as the main contributor to overall mass transfer resistance, being internal transport within the biomass negligible in the studied reactors.

On the other hand, it is important to know how scaling up (especially at great scale) might affect the results obtained. However, lab-scale experiments and modeling are also important for a better knowledge and understanding of the system behavior and helps to find also interesting conclusions for equipment designers. In this case (at lab scale), our aim was to explain whether the effect of pulsation improves the efficiency in this type of bioreactors and the role of both kinetics and mass transfer in this improvement. Thus, in this work it was stated that, in most cases and in both type of reactors, mass transfer resistance has a key role on the enhancement obtained by the application of pulsing flow. Besides, significant differences in the performance between pulsed and nonpulsed bioreactors were obtained. Certainly, at lab scale nonpulsed bioreactors showed typical problems which are of course of higher magnitude at industrial scale. In that sense, it is not possible to extrapolate these results. Flow behavior and mass transfer are not directly scalable parameters and thus a further next research step would be to evaluate the effect of pulsation at higher scale.

Acknowledgments

This work has been supported by the SEDDAN Project (PGIDIT04-TAM265006PR), Xunta de Galicia.

Literature Cited

1. Frankin RJ. Full-scale experiences with anaerobic treatment of industrial wastewater. *Water Sci Technol*. 2001;44:1–6.
2. Young JC, Yang BS. Design considerations for full scale anaerobic filters. *J Water Pollut Control Fed*. 1989;61:1576–1587.
3. Lettinga G, van Velsen AF, Hobma SW, de Zeeuw W, Klapwyk A. Use of the upflow sludge blanket (USB) reactor concept for biological wastewater treatment especially for anaerobic treatment. *Biotechnol Bioeng*. 1980;22:699–734.
4. Grobicki A, Stuckey DC. Performance of the anaerobic baffled reactor under steady-state and shock loading conditions. *Biotechnol Bioeng*. 1990;37:344–355.
5. Alibhai KRK, Forster CF. Physicochemical and biological characteristics of sludges produced in anaerobic sludge blanket reactors. *Enzyme Microb Technol*. 1986;8:601–606.
6. Dolfing J. Kinetics of methane formation by granular sludge at low substrate concentration. The influence of mass transfer limitation. *Appl Microbiol Biotechnol*. 1985;22:77–81.
7. Kitsos HM, Roberts RS, Jones WJ, Tornabene TG. An experimental study of mass diffusion and reaction rate in an anaerobic biofilm. *Biotechnol Bioeng*. 1992;39:1141–1146.
8. Wu MM, Criddle CS, Hickey RF. Mass transfer and temperature effects on substrate utilization in brewery granules. *Biotechnol Bioeng*. 1995;46:465–475.
9. Brito AG, Melo LF. Operation of UASB and EGSB reactors: a simplified analysis of reaction and mass transfer rate. *Environ Technol*. 1997;18:35–44.
10. González-Gil G, Seghezzo L, Lettinga G, Kleerebezem R. Kinetics and mass-transfer phenomena in anaerobic granular sludge. *Biotechnol Bioeng*. 2001;73:125–134.
11. Schmidt JE, Ahring BK. Acetate and hydrogen metabolism in intact and disintegrated granules from an acetate-fed, 55 °C, UASB reactor. *Appl Microbiol Biotechnol*. 1991;35:681–685.
12. de Beer D, Huisman JW, van den Heuvel JC, Ottengraf SPP. The effect of pH profiles in methanogenic aggregates on the kinetics of acetate conversion. *Water Res*. 1992;26:1329–1336.
13. Christiansen P, Hollesen L, Harremoës P. Liquid film diffusion on reaction rate in submerged biofilters. *Water Res*. 1995;29:947–952.
14. Henze M, Harremoës P. Anaerobic treatment of wastewater in fixed film reactors. *Water Sci Technol*. 1983;15:1–101.
15. Pavlostathis SG, Giraldo-Gómez EG. Kinetics of anaerobic treatment. *Water Sci Technol*. 1991;24:35–59.
16. Kato MT, Field JA, Versteeg P, Lettinga G. Feasibility of expanded granular sludge bed reactors for the anaerobic treatment of low strength soluble wastewaters. *Biotechnol Bioeng*. 1994;44:469–480.
17. Zaiat M, Vieira LGT, Foresti E. Liquid-phase mass transfer in fixed-bed of polyurethane foam matrices containing immobilized anaerobic sludge. *Biotechnol Tech*. 1996;10:121–126.
18. Alphenaar PA, Pérez MC, van Berkel WJH, Lettinga G. Determination of the permeability and porosity of anaerobic sludge granules by size exclusion chromatography. *Appl Microbiol Biotechnol*. 1992; 36:795–799.
19. Alphenaar PA, Pérez MC, Lettinga G. The influence of substrate transport limitation on porosity and methanogenic activity of anaerobic sludge granules. *Appl Microbiol Biotechnol*. 1993;39:276–280.
20. González-Gil G, Lens PNL, van Aelst A, van As H, Versprille AI, Lettinga G. Cluster structure of anaerobic aggregates of an expanded granular sludge bed reactor. *Appl Environ Microbiol*. 2001;67:3683–3692.
21. MacLeod FA, Guiot SR, Costerton JW. Layered structure of bacterial aggregates produced in an upflow anaerobic sludge bed and filter reactor. *Appl Environ Microbiol*. 1990;56:1598–1607.
22. Schmidt JE, Ahring BK. Granular sludge formation in upflow anaerobic sludge blanket (UASB) reactors. *Biotechnol Bioeng*. 1996;49: 226–246.
23. Lemay Y, Pineault G, Ruether JA. Particle-liquid mass transfer in a three-phase fixed bed reactor with concurrent flow in the pulsing regime. *Ind Eng Chem Process Des Dev*. 1975;14:280–285.
24. Lerou JJ, Glasser D, Luss D. Packed bed liquid phase dispersion in pulsed gas-liquid downflow. *Ind Eng Chem Fundam*. 1980;19:66–71.
25. Boelhouwer JG, Piepers HW, Drinkenburg AAH. Particle-liquid heat transfer in trickle-bed reactors. *Chem Eng Sci*. 2001;56:1181–1187.
26. Serieys M, Goma G, Durand G. Design and oxygen-transfer potential of a pulsed continuous tubular fermentor. *Biotechnol Bioeng*. 1978;20:1393–1406.
27. Ghommidh C, Navarro JM, Durand G. A study of acetic acid production by immobilized Acetobacter cells: oxygen transfer. *Biotechnol Bioeng*. 1982;24:605–617.
28. Murakami T, Usui J, Takamura K, Yoshikawa T. Application of immersed-type membrane separation activated sludge process to municipal wastewater treatment. *Water Sci Technol*. 2000;41:295–301.
29. Franco A, Gresia G, Roca E, Rozzi A, Lema JM. Influence of pulsation on start-up of UASB reactors. *Water Sci Technol*. 2002;45:163–168.
30. Franco A, Roca E, Lema JM. Improvement of the properties of granular sludge in UASB reactors by flow pulsation. *Water Sci Technol*. 2003;48:51–56.
31. Franco A, Roca E, Lema JM. Enhanced start-up of upflow anaerobic filters by pulsation. *J Environ Eng*. 2007;133:186–190.
32. Lema JM, Núñez MJ, Sanromán A, Roca E. Pulsation device for fermentative, enzymative or chemical reactors. *Spanish Patent* 2059228, 1995.
33. Sekiguchi Y, Kamagata Y, Nakamura K, Ohashi A, Harada H. Fluorescence in situ hybridisation using 16S rRNA-targeted oligonucleotides reveals localization of methanogens and selected uncultured bacteria in mesophilic and thermophilic granules. *Appl Environ Microbiol*. 1999;65:1280–1288.
34. Jeison D, Chamy R. Novel technique for measuring the size distribution of granules from anaerobic reactors for wastewater treatment. *Biotechnol Tech*. 1998;12:659–662.
35. Chu CP, Tsai DG, Lee DJ, Tay JH. Size-dependent anaerobic digestion rates of flocculated activated sludge: role of intrafloc mass transfer resistance. *J Environ Manage*. 2005;76:239–244.
36. Perry RH, Chilton CC. *Chemical Engineers Handbook*, 50th ed. New York: McGraw-Hill, 1985.

37. Beyenal H, Lewandowski Z. Combined effect of substrate concentration and flow velocity on effective diffusivity in biofilms. *Water Res*. 2000;34:528–538.
38. Yang S, Lewandowski Z. Measurement of local mass transfer coefficient in biofilms. *Biotechnol Bioeng*. 1995;48:733–744.
39. Ohashi A, Harada H. Adhesion strength of biofilm developed in an attached growth reactor. *Water Sci Technol*. 1994;29:281–288.
40. Bailey JE, Ollis DF. *Biochemical Engineering Fundamentals*, 2nd ed. New York: McGraw-Hill, 1986.
41. Mohan SV, Babu VL, Bhaskar YV, Sarma PN. Influence of recirculation on the performance of anaerobic sequencing batch biofilm reactor (AnSBBR) treating hypersaline composite chemical wastewater. *Bioresour Technol*. 2007;98:1373–1379.
42. Batstone DJ, Keller J. Variation of bulk properties of anaerobic granules with wastewater type. *Water Res*. 2001;35:1723–1729.
43. Fukuzaki S, Nishio N, Nagai S. Chemical composition and kinetic properties of granular methanogenic sludge grown on propionate. *J Ferment Bioeng*. 1991;72:405–407.
44. Beyenal H, Lewandowski Z. Internal and external mass transfer in biofilms grown at various flow velocities. *Biotechnol Prog*. 2002; 18:55–61.
45. Brito AG, Melo LF. Mass transfer coefficients within anaerobic biofilms: effects of external liquid velocity. *Water Res*. 1999;33:3673–3678.
46. Wittler R, Baumgartl H, Lübbers DW, Schügerl K. Investigations of oxygen mass transfer into *Penicillium chrysogenum* pellets by microprobe measurements. *Biotechnol Bioeng*. 1986;28:1024–1036.
47. de Beer D, Stoodley P, Lewandowski Z. Liquid flow and mass transport in heterogeneous biofilms. *Water Res*. 1996;30:2761–2765.
48. van den Heuvel JC, Beuling EE, van Dusschoten D, Roosenschoon OL, Verschuren PG. Convective flow in methanogenic granules. *Water Sci Technol*. 1997;36:311–316.
49. Roca E, Flores J, Núñez MJ, Lema JM. Ethanolic fermentation by immobilized *Saccharomyces cerevisiae* in a semipilot pulsing packed-bed bioreactor. *Enzyme Microbial Technol*. 1996;19:132–139.
50. Franco A, Roca E, Lema JM. Granulation in high-load denitrifying upflow sludge bed (USB) pulsed reactors. *Water Res*. 2006;40:871–880.

Manuscript received Aug. 1, 2007, and revision received Jan. 10, 2008.